

Shrinkage of Satopanth and Bhagirath Kharak Glaciers, India, from 1936 to 2013

H.C. NAINWAL,¹ Argha BANERJEE,^{2*} R. SHANKAR,³ Prabhat SEMWAL,¹
Tushar SHARMA¹

¹HNB Garhwal Central University, Srinagar (Garhwal), Uttarakhand, India

²Indian Institute of Science Education and Research Kolkata, Mohanpur, India

³The Institute of Mathematical Sciences, Chennai, India

Correspondence: H.C. Nainwal <nainwalhc@yahoo.co.in>

ABSTRACT. We have compiled and analysed available records and data on the shrinkage of Satopanth (SPG) and Bhagirath Kharak (BKG) Glaciers, Uttarakhand, India, during the period 1936–2013. We estimate the mean retreat rates of the snouts of SPG and BKG for this period at $9.7 \pm 0.8 \text{ m a}^{-1}$ and $7.0 \pm 0.6 \text{ m a}^{-1}$ respectively. We have also revised the estimates of the area vacated during the period 1956–2013 to be $0.27 \pm 0.05 \text{ km}^2$ and $0.17 \pm 0.04 \text{ km}^2$ for SPG and BKG respectively, corresponding to front-averaged retreat rates of $5.7 \pm 0.6 \text{ m a}^{-1}$ and $6.0 \pm 0.9 \text{ m a}^{-1}$. The study revealed an average thinning of glacial ice in the lower ablation zone of SPG of $9 \pm 11 \text{ m}$ in the past 51 years. We observed that while the fronts of SPG and BKG depicted in the Survey of India topographic map published in 1962 are inconsistent with other available records, the elevation contours are consistent with them.

KEYWORDS: climate change, debris-covered glaciers, glacier fluctuations

INTRODUCTION

The response of Himalayan glaciers to the rapidly warming climate is an important issue, as they feed rivers that sustain almost 800 million people living in Himalayan mountains and in the Indo-Gangetic Plain (Immerzeel and others, 2010). Quantitative projections for the future require good data about the past (Oerlemans, 2005). Unfortunately, such data are scarce for glaciers in the Indian Himalaya.

During the past two decades a number of remote-sensing and field studies have been carried out on glacier fluctuations in the Himalaya. In many of these studies, 1962 Survey of India (SOI, 1962) topographic maps have been used as a baseline for estimation of area and length changes. Thereafter, more or less regular data are available from the end of the 20th century, often because of the availability of good quality satellite images. However, the reliability of glacier extents derived from the SOI topographic maps has been questioned (Vohra, 1980; Raina and Srivastava, 2008; Bhambri and Bolch, 2009; Raina, 2009). Thus, there is clearly a need for concerted efforts to collate existing scattered information on recent glacial extents of various glaciers in the Indian Himalaya and also to cross-check SOI topographic map glacier fronts with independent measurements whenever they are available. In this paper, we describe our attempt to perform this task for two important glaciers in the Indian Himalaya: Satopanth (SPG) and Bhagirath Kharak (BKG) Glaciers.

These are two relatively well-studied glaciers as far as length fluctuation is concerned. There has been a study of the palaeo-glaciation (Nainwal and others, 2007) and several studies of length and front area changes (Jangpangi, 1956; Sangewar, 2000; Nainwal and others, 2008; Raina and others, 2015). A systematic study incorporating all these data is lacking.

One motivation for synthesizing the past data is to develop glacier models (Adhikari and Huybrechts, 2009) which can be used to predict future changes. A major obstacle in understanding Himalayan glaciers is the abundance of glaciers with thick supraglacial debris cover. Remote-sensing (Scherler and others, 2011) and modelling (Banerjee and Shankar, 2013) studies indicate that glaciers with a thick debris cover respond differently to a warming climate, as compared to debris-free glaciers. Debris-free glaciers approximately retain their shape (thickness profile), so changes in their length reflect changes in their volume. On the other hand, debris-covered glaciers change shape in response to warming and there is considerable thinning in the lower ablation zone, so the length changes do not necessarily reflect the ice volume loss (Banerjee and Shankar, 2013). Hence, for debris-covered glaciers like SPG and BKG there is a need to study thickness changes in the lower ablation zone as well, in order to validate models. We have therefore studied the shrinkage of these two glaciers, i.e. their reduction in all dimensions. We study the length changes of both glaciers and the thickness changes in the last 8 km of SPG and the last 1 km of BKG.

We use accounts and maps produced by past explorers in the region, published records, satellite images and our own field data to obtain a coherent picture of the shrinkage of the twin glaciers. We attempt to reconstruct both the front variations and the thinning rates in the lower ablation zone over the past eight decades. We also investigate the accuracy of the SOI (1962) topographic map boundaries for these glaciers and revise the previously reported retreat rates of the twin glaciers (Nainwal and others, 2008).

SATOPANTH AND BHAGIRATH KHARAK GLACIERS

The east–west-trending SPG (21 km²) and BKG (31 km²) are approximately 13 and 18.5 km long with an average width of

*Present address: Indian Institute of Science Education and Research, Pune, India.

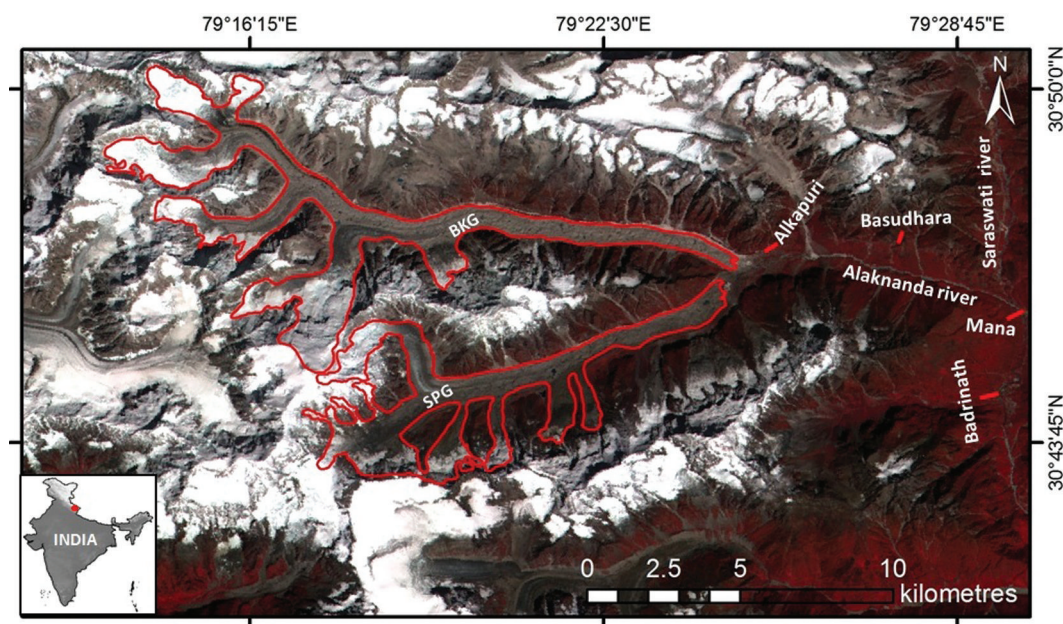


Fig. 1. Satopanth and Bhagirath Kharak Glaciers. The red spot in the inset shows the location in India.

about 750 and 850 m respectively (Fig. 1). The ablation zones of both glaciers are covered by a thick layer of debris. The snouts of SPG and BKG are located at 3858 and 3796 m a.s.l. respectively. The Alaknanda river originates from SPG and meets Uttar Ganga (meltwater channel of BKG) upstream of Alkapuri. At Mana, Alaknanda meets Saraswati river and from there onwards flows as a braided meandering river in Badrinath basin. After leaving Badrinath basin, it becomes a torrential cascading river that has carved a deep gorge in the crystalline rocks (Nainwal and others, 2007).

The Upper Alaknanda basin falls under the Higher Himalayan zone, described as the Himadri Complex by Valdiya (1973) and Valdiya and others (1999). The area is underlain by calc-silicate gneiss and schist with granitic intrusions.

DATA SOURCES

The data sources are given in Table 1. We were able to extract quantitative information from some of them, as detailed in the next section. Here we summarize the qualitative information contained in the sources. Mumm

Table 1. Data sources

No.	Source	Type of data
1	Mumm (1909)	Travel account
2	Smythe (1932a)	Travel account
3	Smythe (1932b)	Report and 1 : 500 000 map
4	Shipton (1935)	Report and 1 : 250 000 map
5	Heim and Gansser (1939)	Report and barometric snout elevations
6	US Army (1954)	1 : 250 000 topographic map
7	Jangpangi (1956)	1 : 5000 survey map
8	SOI (1962)	1 : 50 000 topographic map
9	Corona, 24 Sept 1965	Satellite image, 2.5 m resolution
10	Raina and others (2015)	1 : 5000 survey map
11	Landsat ETM+, 15 Oct 1999	Satellite image, 30 m resolution
12	Current study	DGPS glacier surface survey, June 2013
13	Current study	DGPS outwash plain survey, May 2014

(1909) indicated that in 1909 the glaciers were united. The accounts of Smythe (1932a,b), Shipton (1935) and the US Army (1954) topographic map are somewhat ambiguous, but Heim and Gansser (1939) clearly indicate that the glacier fronts were separated during their 1936 expedition. They also observed that the lateral moraine crests were about 10–25 m above the glacier surface, indicating thinning in the lower ablation zone. The map of Jangpangi (1956) shows well-separated fronts. However, the SOI (1962) topographic map shows a united front.

METHODOLOGY

In what follows, the term ‘front’ refers to the ice boundary across the valley where the glacier terminates, and ‘snout’ refers to the point on the front where the stream emanates. In this section, we describe the methodology adopted to reconstruct: (1) the retreat of the snout, (2) the area vacated in the front region and (3) the thickness changes in the lower ablation region. We also analyse the uncertainties involved in our reconstruction.

The 1 : 250 000 sketch map of Shipton (1935), when geo-referenced, showed glacier boundaries, streams, etc., which were inconsistent with other maps mentioned in the previous section. This is not surprising as the scale of the sketch map is very coarse, and the map cannot be used for accurately locating small-scale features in which we are interested. For similar reasons, we did not use the map of Smythe (1932b) or the US Army (1954) topographic map.

Length and area changes

A Trimble R6 differential GPS (DGPS) was utilized to map the glacier snout position and front boundary in 2013. Google Earth was used to obtain front boundaries and snout positions in 2005. We mapped the 1999 snouts from a geo-referenced Landsat Enhanced Thematic Mapper Plus (ETM+) image. The front boundaries could not be marked accurately, as the pixel size of the Landsat image is 30 m. We geo-referenced and processed the 1965 Corona image using ArcGIS software, taking the SOI (1962) topographic map as the base map. We

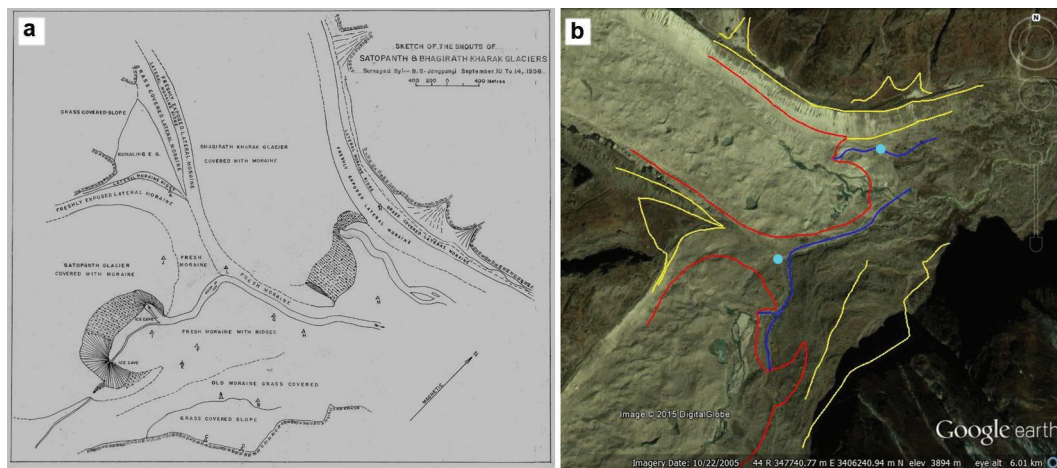


Fig. 2. (a) The original Jangpangi (1956) map. (b) Some digitized features of the stretched map overlaid on the Google Earth image. The yellow lines are moraine ridges and fans. The dark blue lines are the streams. The light blue dots show the estimated snout positions in 1936. The red lines are the glacier front boundaries in 1956.

could not do the orthorectification since we had only one Corona image. We discuss the errors caused by this further below. The geo-referenced 1965 Corona image was used to demarcate the boundaries of the glaciers. The thick debris cover makes the task difficult. We were able to mark out the boundary of SPG with relative accuracy due to the presence of exposed ice faces. Unfortunately, such features were absent in BKG in 1965, making the boundary uncertain, so we could not produce a reliable front from the Corona image for BKG. The snouts of both glaciers were located accurately from the 1965 Corona image.

Our attempts to geo-reference Jangpangi's (1956) map using a small number of identifiable fixed features were not productive. The resultant geo-referenced map has many inconsistencies with other maps as far as positions of glacier boundaries, moraines, etc., are concerned. But given the detailed nature of the map, and that we do not have any other data available for the period, we took a non-standard approach: we superimposed the map on the Google Earth image so that the fixed features (e.g. moraines, cliffs, streams, debris fans, etc.) across the whole map are approximately matching. To achieve this, we had to stretch the map by ~5% along the northeast direction. The original map is shown in Figure 2a. The outlines of features in the stretched map that we matched, moraine ridges, fans and streams, overlaid on the 2005 Google Earth image, are shown in Figure 2b.

Heim and Gansser (1939) report barometric measurements of the snout elevations of SPG and BKG, taken in their 1936 expedition, to be 3800 and 3750 m respectively. We have located the snout positions in 1936 by identifying the points with these elevations in the palaeo-channels visible in the Google Earth image as shown in Figure 2b. The front boundaries and snout positions at different times superposed on the 1965 Corona image are shown in Figure 3.

There are two sources of uncertainty in our estimates. Firstly, there are what we will refer to as measurement errors which are due to the imperfections of the measuring process. Secondly, there are co-registration errors due to the fact that we are estimating the changes by comparing data from different sources and their coordinate systems will typically not be exactly matched. The total uncertainty of the measured coordinates of the features is the square root of the sum of the squares (rss) of these two errors.

We first discuss the measurement errors. The instrument accuracy of the DGPS is very high, with errors <1 cm. The accuracy of the satellite-based measurements is determined by the pixel size. The 2005 Google Earth and the 1965 Corona images have pixel sizes 2.5 m, and the 1999 Landsat image pixel size is 30 m. The Jangpangi (1956) map and the Raina and others (2015) map are based on field surveys. We therefore expect the instrument errors to be quite small, of the order of a few centimetres.

However, there are other sources of uncertainty. Firstly, due to the width of the stream, the snout position is ambiguous by a couple of metres. The ice boundaries have an intrinsic width. Even when there is a cliff at the front, it is not vertical and can have a width in excess of 20 m. In addition, much of the front is completely covered with debris. In satellite images (Basnett and others, 2013) and even in the field it is impossible to determine the exact location of the ice boundary in these regions, so, in the field, the boundary is guessed by interpolating between the portions of exposed ice and seeing where there is a sharp

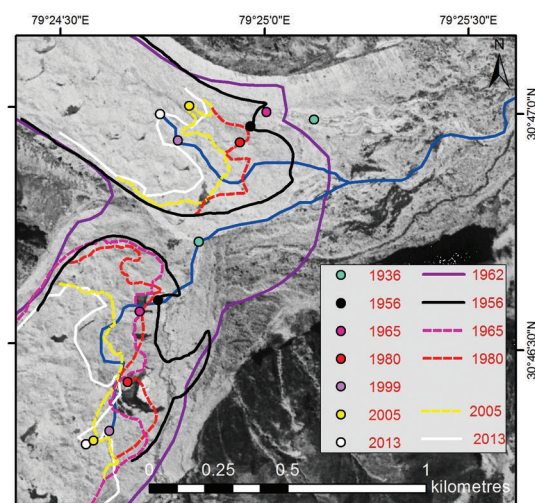


Fig. 3. The front boundaries and snout positions at different times superposed on the 1965 Corona image. Bandhara stream can be seen near the zero of the scale.



Fig. 4. An illustration of the intrinsic uncertainties in the boundary. The two red lines mark possible locations of the boundary of SPG in a 2005 Google Earth image. The regions marked 1 are completely debris-covered, making it impossible to pinpoint the ice boundary even in the field. 2 shows the finite width of the ice cliff discussed in the text.

increase in elevation. Based on our experience, we estimate that there is an intrinsic uncertainty of about ± 10 m in the boundary determined by this procedure. Figure 4 made from the Google Earth image of 2005 illustrates these issues.

We take our measurement error to be the rss of the instrument/image resolution and the intrinsic uncertainty associated with the feature, ± 10 m for the front coordinates and ± 2 m for the snout coordinates.

Heim and Gansser (1939) do not report the uncertainties of their barometric measurements of the snout elevations. There is no systematic way to estimate this uncertainty since it depends on the measurement conditions, so we have guessed it to be ± 20 m. The corresponding range of elevations leads to uncertainties in the position along the valley of about ± 150 m for both glaciers.

Next, we estimate the co-registration errors. The DGPS instrument accuracy is very high, so we take the DGPS coordinates to be virtually exact in the WGS84 coordinate system. To assess the uncertainties of the coordinates of the other satellite images with respect to the DGPS coordinates, we compared the horizontal coordinates (latitude–longitude) of ten prominent fixed features (e.g. large boulders, the corner of a building, bridges, etc.) spread from ~ 10 km downstream to ~ 5 km upstream of the snout, as obtained from the different sources we are using.

First, we compared the coordinates of these ten features in the Google Earth images of 2005, 2011 and 2014. We calculated the mean coordinates of each feature and the root mean square (rms) of the deviations from the mean. We found the rms of the deviation to be $\Delta_G = 3.5$ m for both the northing and the easting. We interpret this spread to be the rss of the pixel size and the co-registration error with respect to the (virtually exact) DGPS coordinates. The co-registration error is hence $\sqrt{3.5^2 - 2.5^2} = 2.45 \approx 2.5$ m.

We then found the rms of the deviations of the 1965 Corona and Google Earth coordinates for these ten features to be 8.5 m for both coordinates. We interpret this spread to be the rss of the Δ_G and the uncertainty in the Corona

Table 2. Sources and rounded uncertainties in the snout positions and front boundaries. Δ_{CR} is the co-registration error, Δ_M the measurement error and Δ the total uncertainty

Year	Source	Snout positions			Front boundaries	
		Δ_{CR} m	Δ_M m	Δ m	Δ_M m	Δ m
1936	Heim and Gansser (1939)	–	150	150	–	–
1956	Jangpangi (1956)	17	2	17	10	20
1965	Corona image	7.5	3	8	10	13
1980	Raina and others (2015)	17	2	17	10	20
1999	Landsat image	$\ll 30$	30	30	–	–
2005	Google Earth	2.5	3	4	10	11
2013	DGPS survey	0	2	2	10	10

coordinates, Δ_C . We thus get $\Delta_C = \sqrt{8.5^2 - 3.5^2} = 7.75 \approx 8$ m. The uncertainty in the Corona coordinates is the rss of the pixel size and the co-registration error. Thus the co-registration error is $\sqrt{7.75^2 - 2.5^2} = 7.33 \approx 7.5$ m. This will include the error caused by the lack of orthorectification. There was also an offset of 5 m in the northing and -0.4 m in the easting, but since these are significantly smaller than the spread we neglect them.

The rms of the deviations of the 1999 Landsat and the Google Earth coordinates for these ten features was ~ 25 m for both coordinates. Since this is around the same as the pixel size, we conclude that the co-registration error is $\ll 30$ m. Again, the offsets (4.8 m, 2.8 m) were smaller than the spread.

The Jangpangi (1956) map and the Raina and others (2015) map are co-registered, so the following uncertainty estimates are for both. We have compared the coordinates of six fixed features of the Jangpangi (1956) map after our stretching procedure and Google Earth image. The rms of the deviations was found to be 14 m for the easting and 17 m for the northing. We take the uncertainty in both coordinates to be 17 m and estimate the co-registration error to be $\sqrt{17^2 - 3.5^2} = 16.6 \approx 17$ m.

The measurement errors, co-registration errors and the total uncertainties of the coordinates of the front boundaries and snout positions are given in Table 2.

The retreat or advance of the glacier front is one of the indicators of ice loss or gain. The front may change its shape as it retreats, so different parts of it could retreat at different rates. The average rate of retreat is the area loss divided by the width and we refer to this quantity as the front-averaged retreat rate. The snout is one point on the front. At very long timescales, the average retreat rates of all points on the front have to be almost the same (otherwise the front boundary will keep getting stretched in the valley direction), so the front average retreat rate and the snout retreat rate have to be the same over very long time periods. However, over shorter periods, this is not true and two retreat rates can differ (Moon and Joughin, 2008).

The snout position changes both along the valley and in the cross-valley direction. To measure the snout retreat rates, we have projected the positions in the valley direction so that we measure the retreat rates along the valley. These coordinates are plotted in Figure 6 and the uncertainties in the projected positions are given in Table 2. The average retreat rate over the period 1936–2013 is estimated as the

slope of the best-fit straight line computed by the least-squares method where the sum of individual squared deviations, inversely weighted by corresponding squared uncertainties, is minimized. The retreats for the different intervals are tabulated in Table 3. The uncertainty of the retreat between two times is computed as the rss of the uncertainties of the snout positions at those two times.

We estimate the area changes from a particular time to 2013 by measuring the area enclosed by the front boundaries at that time and in 2013. The uncertainties in the areas are calculated by measuring the perimeter of the region enclosed by the two boundaries and multiplying it by the uncertainty in the boundary tabulated in Table 2. The front average retreat between the two times is the area change, A , divided by the width of the glacier, W , in the front region. We measured widths of 720 ± 20 m and 510 ± 20 m for SPG and BKG respectively. The uncertainties in the front average changes are computed using the formula for the uncertainty of a function of two variables, $f(x_1, x_2)$, $\Delta f = \sqrt{(\partial f/\partial x_1)^2 \Delta_{x_1}^2 + (\partial f/\partial x_2)^2 \Delta_{x_2}^2}$, where $\Delta_{x_{1(2)}}$ is the uncertainty in $x_{1(2)}$. We compute the uncertainty in the change in the front positions by putting $x_1 = A, x_2 = W$ and $f(A, W) = A/W$ in the above formula.

Thickness changes

We measured the thickness changes in the lower ablation zone of the glaciers during the period 1962–2013 using DEMs made from the SOI (1962) topographic map and the DGPS field survey of the glacier surface in June 2013.

To estimate the offset and uncertainty between the SOI elevations and the DGPS elevations, we compared their elevations at 20 points in the outwash plain, extending to ~1.5 km downstream of the 1956 boundary. The DGPS elevations were obtained from the survey conducted in May 2014. We subtracted the SOI (1962) DEM elevations from the 2014 DGPS elevations and calculated the mean and standard deviation of the elevation changes. The mean was found to be -27 m and the standard deviation 11 m, which we take as the offset and uncertainty respectively. The offset is consistent (within uncertainties) with the fact that the WGS84 ellipsoid datum (of the DGPS) is higher than the Everest-1830 datum (of the SOI (1962) topographic map) in our study region by ~23 m (Ghosh and Dubey, 2008).

We estimate the thickness changes in the lower ablation zones of SPG and BKG from 1962 to 2013 by first subtracting the offset of 27 m from the 1962 SOI DEM and then subtracting the 1962 SOI DEM from the 2013 DGPS DEM.

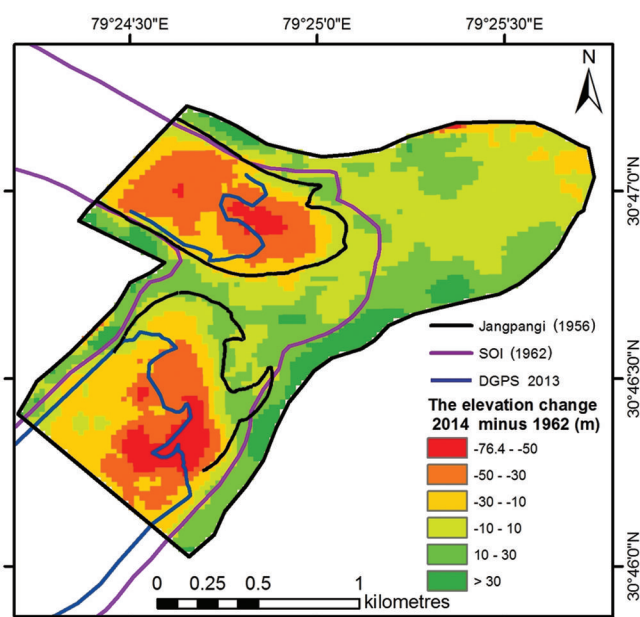


Fig. 5. The elevation change obtained by subtracting the DEM made from the 1962 SOI topographic map from the DEM made from the 2013 and 2014 DGPS surveys.

Accuracy of the SOI topographic map

Figures 3 and 5 show that the SOI (1962) united front boundaries SPG and BKG are inconsistent with our other sources. If taken to be accurate, it implies that SPG advanced by a few hundred metres in the 6 year interval 1956–62. Such a rapid advance would imply that SPG is a surge-type glacier. Since there is no other evidence of this, we reject this interpretation.

While geo-referencing the Corona image with the SOI (1962) map as the reference, the co-registration errors were <1 m. Also, as described in the previous subsection, the elevations of fixed points of the SOI (1962) map are consistent with field measurements within ~10 m. Thus, the evidence seems to support the statement of Raina (2009) that while the accuracy of the ‘other physical features ... is exceptionally high’ there are inaccuracies in the glacier front boundaries as the maps were based on aerial photographs taken during November–January when it becomes difficult to differentiate between the actual glacier front and the snow-covered terminal moraines.

Table 3. Snout and front retreat rates and the area vacated during the different periods

Period	Satopanth Glacier			Bhagirath Kharak Glacier		
	Snout retreat rate m a ⁻¹	Front retreat rate m a ⁻¹	Area vacated km ²	Snout retreat rate m a ⁻¹	Front retreat rate m a ⁻¹	Area vacated km ²
1936–56	13.3 ± 7.5	–	–	9.5 ± 7.5	–	–
1956–65	9.5 ± 2.1	17.0 ± 9.7	0.11 ± 0.06	-2.0 ± 2.1	–	–
1965–80	13.7 ± 1.3	0.0 ± 5.8	0.00 ± 0.06	1.2 ± 1.3	–	–
1956–80	12.1 ± 1.0	6.4 ± 4.1	0.11 ± 0.05	0.0 ± 1.0	6.5 ± 4.1	0.08 ± 0.05
1980–99	9.2 ± 1.8	–	–	10.8 ± 1.8	–	–
1999–2005	11.8 ± 3.80	–	–	7.5 ± 3.8	–	–
1980–2005	9.8 ± 0.7	7.2 ± 3.0	0.13 ± 0.05	10.0 ± 0.7	3.1 ± 2.8	0.04 ± 0.03
2005–13	4.1 ± 0.6	5.2 ± 3.7	0.03 ± 0.02	9.1 ± 0.6	12.2 ± 5.0	0.05 ± 0.02

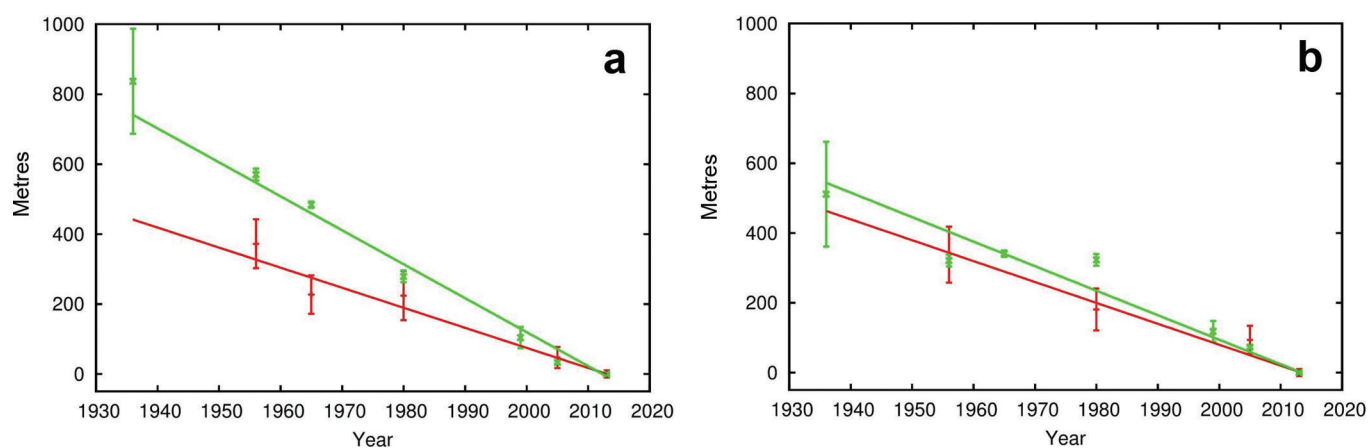


Fig. 6. Changes in snout positions with respect to 2013 (green), and changes in average front positions with respect to 2013 (red). The best-fit straight lines are also shown. (a) SPG; (b) BKG.

To investigate this further, we made a DEM combining the glacier surface points from the 2013 DGPS survey extending to ~ 0.5 km upstream of the current fronts and the points of the 2014 DGPS survey of the outwash plain extending to ~ 1.5 km downstream of the 1956 fronts. The SOI (1962) DEM was subtracted from this DEM after accounting for the offset. The result is shown in Figure 5 which indicates that the elevations have not changed much in the region downstream of the 1956 fronts. The thinning starts in the vicinity of the 1956 fronts and increases rapidly in the upstream direction. We interpret this thinning as due to the melting of the glacier ice from 1962 to 2014. The lack of thinning in the region between the 1956 fronts and the 1962 SOI front is consistent with the interpretation that this region was snow-covered in 1962.

Based on the above discussion, we conclude that while the united glacier front outlines of SPG and BKG depicted in the SOI (1962) map are inconsistent with our other sources, their contours and the coordinates of other features are consistent with them.

RESULTS AND DISCUSSION

Snout retreat

Our estimates of the snout recessions, area vacated and average front recessions during different periods for the two glaciers are given in Table 3.

The snout positions are plotted in Figure 6. During the period 1936–2013, the SPG snout has retreated by 837 m measured along the valley, with a corresponding increase in snout elevation of 58 m. For the same period, the BKG snout retreated by 511 m (Fig. 6) and its elevation increased by 46 m. The average snout retreat rates (defined as the negative of the rate of change of length), during this period, calculated from the slope of the best-fit straight lines to each time series, are $9.7 \pm 0.8 \text{ m a}^{-1}$ for SPG and $7.0 \pm 0.6 \text{ m a}^{-1}$ for BKG.

The revised retreat rates we report here are different from those reported in Nainwal and others (2008) for the period 1962–2005, which were 22.9 m a^{-1} for SPG and 7.4 m a^{-1} for BKG. The main reason for this revision is that the front outlines of the SOI (1962) map were used in Nainwal and others (2008). As can be seen in Figures 3 and 5, this affects SPG much more than BKG, so the difference in the two rates has come down and is consistent with both glaciers experiencing the same warming climate.

The snout retreat rate of SPG is significantly larger than that of BKG even after the revision. We attribute this to the fluvial action of Bandhara stream that drains a significant portion of the right lateral basin of SPG and meets the glacier in this region (Nainwal and others, 2008). The fact that there is more retreat of the SPG front on the right margin, where Bandhara stream joins the glacial meltwater channel (Figs 3 and 4), supports our hypothesis. Further, since the snout retreated upstream of the Bandhara confluence ~ 8 years ago, its retreat rate has decreased to $\sim 4.1 \text{ m a}^{-1}$ (Table 3).

Area loss and front retreat

From 1956 to 2013, SPG and BKG have vacated $0.27 \pm 0.05 \text{ km}^2$ and $0.17 \pm 0.04 \text{ km}^2$ respectively, corresponding to average rates of $4736 \pm 875 \text{ m}^2 \text{ a}^{-1}$ and $2982 \pm 700 \text{ m}^2 \text{ a}^{-1}$. Based on Corona and Advanced Spaceborne Thermal Emission and Reflection Radiometer (ASTER) imagery, Bhambri and others (2011) report that from 1968 to 2006 SPG lost 0.28 km^2 near the snout, whereas BKG lost only 0.083 km^2 , corresponding to average rates of 7368 and $2184 \text{ m}^2 \text{ a}^{-1}$. Thus our rates are ~ 1.5 times smaller for SPG, and ~ 1.5 times larger for BKG, than the rates reported by Bhambri and others (2011). The reason for this discrepancy is being investigated.

We have plotted front positions with respect to the 2013 position in Figure 6 for both glaciers. The average front retreat rates are $5.7 \pm 0.6 \text{ m a}^{-1}$ for SPG and $6.0 \pm 0.9 \text{ m a}^{-1}$ for BKG. These are smaller than the snout retreat rates. In SPG and BKG much of the front boundaries are under a thick debris cover. For much of the period during which we have observed the snouts of the two glaciers, they were located at regions of exposed ice face/cliff/cave (Figs 2 and 4). This will increase the melt rate locally (Basnett and others, 2013), making the snout retreat faster than, and hence causing an overestimate of, the average for the front as a whole. This may be a general trend in thickly debris-covered glaciers responding to a warming climate. We argued earlier that over very long periods the two rates have to be almost the same. Our results indicate that this 'very long period' may be much more than 76 years.

The front average retreat of the two glaciers over the past 57 years is almost the same (within uncertainties), which is consistent with the fact that they are responding to a similar warming climate.

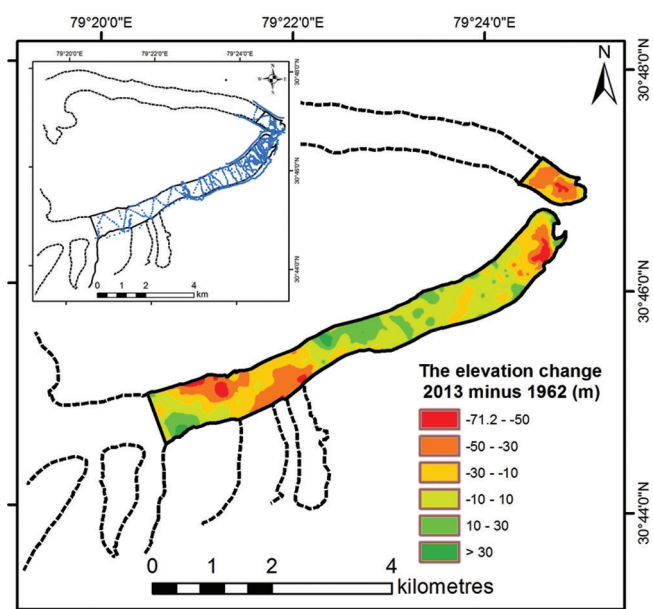


Fig. 7. The elevation change obtained by subtracting the DEM made from the SOI (1962) map from the DEM made from the 2013 DGPS survey for the last 8 km of SPG and last 1 km of BKG. The inset shows the locations of the DGPS points used to make the 2013 DEM.

Thickness changes

The average thinning for SPG in the last 8 km from 1962 to 2013 is 9 ± 11 m or 0.17 ± 0.21 m a⁻¹, where ‘thinning’ is defined as the negative of the change of elevation. For the last 1 km of SPG, the thinning is 21 ± 11 m or 0.41 ± 0.21 m a⁻¹. During the same period, for the last 1 km of BKG, the average thinning is 29 ± 11 m or 0.57 ± 0.21 m a⁻¹ (Fig. 7).

The thinning rates of the last 1 km of both glaciers are comparable within the uncertainties, again consistent with both glaciers experiencing the same climate. In SPG, as is clear from Figure 7, the thinning is greater in the front region. There are also regions of local thickening. This may be because, as with many other debris-covered glaciers, the surface in the debris-covered region is highly corrugated. There are humps and depressions of 10–20 m extent in the vertical direction. These move with the ice and can cause local thickening. For instance, if a region with an average thinning of 10 m had a 20 m depression in 1962 and a 10 m hump in 2013, the region will thicken by 10 (hump) – (–20) (depression) – 10 (thinning) = 20 m.

While the uncertainty is high, the thinning rate for the last 8 km of SPG compares well with the available records in other regions of the Himalaya (Dyurgerov and Meier, 2005).

Comparison with nearby glaciers

There is now evidence that, on average, the glaciers in the Himalaya are losing mass at rates similar to those observed elsewhere (Bolch and others, 2012). The warming rate for the second half of the 20th century, extracted from retreat rates of glaciers with very little debris cover, is the same as the global average with a large variability (Banerjee and Shankar, 2013). A temperature reconstruction based on length records of glaciers yields a temperature profile similar to the global average for the second half of the 20th century (Banerjee and Azam, 2016). However, the regional variations in the response of the glaciers are difficult to

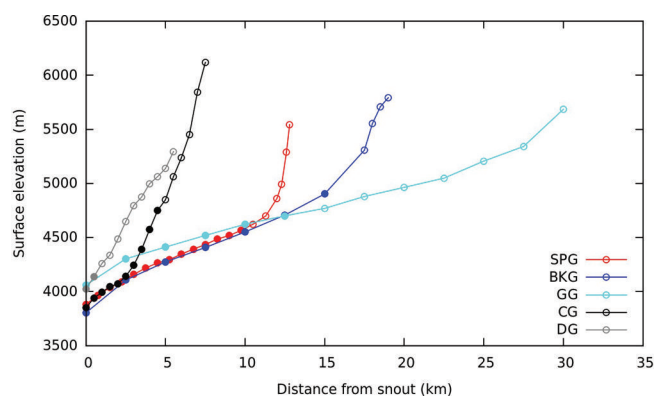


Fig. 8. Surface profiles of the five glaciers. The solid dots indicate debris-covered regions, and the open circles the debris-free regions.

understand (Fujita and Nuimura, 2011) and the response of Himalayan glaciers to global warming has been very aptly compared to a montage (Kargel and others, 2011). Indeed, when viewed through the lens of standard paradigms (Oerlemans, 2001), it is difficult to make a coherent picture of the observed variations (Scherler and others, 2011).

We examine this issue by comparing our results for the average retreat of SPG and BKG with those reported for three nearby glaciers which are relatively well studied in the field: Gangotri (GG; 30.82° N, 79.13° E), Chorabari (CG; 30.77° N, 79.05° E) and Dokriani (DG; 30.85° N, 78.82° E). These glaciers are within 50 km of each other and may be expected to be experiencing a similar climate.

Field studies of retreat rates during the past several decades have been reported for these glaciers. The front of GG has retreated at an average rate of ~ 19 m a⁻¹ from 1935 to 1999 (Srivastava, 2004). Snout retreat rates of CG during 1962–2012 (Dobhal and others, 2013) and DG during 1962–2007 (Dobhal and Mehta, 2010) have been reported to be 6.8 and 15 m a⁻¹ respectively.

We now try to understand the variations in average retreat rates using a paradigm that has been successfully applied at the global scale (Oerlemans, 2005; Leclercq and Oerlemans, 2012), namely that the response of a glacier to changes in climate is largely governed by its geometry (length and slope). A steep glacier is expected to retreat less than a glacier with a gentle slope, and a longer glacier is expected to take more time to adjust to changes in climate. The lengths, slopes and the above-mentioned retreat rates are tabulated in Table 4. The surface profiles of the glaciers, made from Google Earth images, are shown in Figure 8. The

Table 4. Geometry and average retreat rates of the five neighbouring glaciers

Glacier	Length km	Avg. slope °	Avg. retreat rate m a ⁻¹	Period
Gangotri	30.0	2.6	19	1935–99
Chorabari	7.5	16.2	6.8	1962–2012
Dokriani	5.5	13.0	15	1962–2007
SPG	13.0	5.4	5.7	1956–2013
BKG	18.5	5.4	6.0	1956–2013

average slopes have been computed as the slopes of the best-fit straight line.

All these glaciers are retreating, which is consistent with all of them experiencing a warming climate. We see from Table 4 that SPG and BKG have similar geometries and average retreat rates. However, DG and CG also have similar geometries but DG has an average retreat rate more than twice that of CG. The average retreat rates of SPG and BKG are similar to that of CG despite its being about three times steeper. Clearly, the response of these five glaciers to the warming climate is not governed by their lengths and slopes alone.

These glaciers have varying extents of debris cover. The debris-covered region is shown as solid dots in Figure 8. Dokriani is almost free of debris, Gangotri and Chorabari have about half their lengths under debris cover whereas only about 15% of SPG and BKG are free of debris. Further, unlike the other three, the slopes of SPG and BKG rise very sharply in their accumulation regions. The Google Earth images also show very high and steep head walls with large ice-free regions. All this indicates that unlike the other three glaciers, SPG and BKG may be dominantly avalanche-fed.

Thick debris cover may be an important factor in the dynamics (Scherler and others, 2011; Banerjee and Shankar, 2013). The debris is transported by the ice, and hence the debris distribution is strongly influenced by the ice flow. The debris distribution strongly influences the specific mass-balance profile which in turn affects the ice flow pattern.

The data in Table 4 are consistent with the conjecture that an extensive debris cover tends to slow the retreat of the glacier (Kargel and others, 2011). It is possible that the more extensive debris cover of Gangotri explains why its average retreat rate is similar to that of Dokriani. Similarly, it is possible that the more extensive cover of SPG and BKG makes their average retreat rates similar to that of the much steeper Chorabari. Further, the similar average retreat rates of SPG and BKG, which are similar in all respects, i.e. geometry, extent of debris cover and the nature of the accumulation zones, may indicate that these are the three important factors that determine a glacier's response to a warming climate.

The above discussion indicates that to have a quantitative understanding of the Himalayan montage, it is necessary to develop a good model of the strongly coupled debris-ice dynamics. However, we have analysed only one set of five nearby glaciers. It is necessary to repeat the analysis for many more sets before firm conclusions can be drawn.

CONCLUSIONS

We have extended the shrinkage record of SPG and BKG since 1936. Based on several old records and maps, we have presented evidence that while the glacier fronts of SPG and BKG depicted in the SOI (1962) topographic map are inaccurate, the coordinates and elevations are fairly accurate. This has led to revised estimates of the area vacated and snout retreat in the past 57 years. The area vacated from 1956 to 2013 is estimated at $0.27 \pm 0.05 \text{ km}^2$ and $0.17 \pm 0.04 \text{ km}^2$ for SPG and BKG respectively, corresponding to front averaged retreat rates of $5.7 \pm 0.6 \text{ m a}^{-1}$ and $6.0 \pm 0.9 \text{ m a}^{-1}$. The revised snout retreat rates from 1936 to 2013 are $9.7 \pm 0.8 \text{ m a}^{-1}$ for SPG and $7.0 \pm 0.6 \text{ m a}^{-1}$ for BKG. We attribute the larger difference between these rates to the fluvial action of the Bandhara stream. The last 8 km of SPG

shows an average thinning of $9 \pm 11 \text{ m}$ from 1962 to 2013. The mean thinning rates in the last 1 km of SPG and BKG during 1962–2013 are $0.41 \pm 0.21 \text{ m a}^{-1}$ and 0.57 ± 0.21 respectively.

While these results are consistent with SPG and BKG experiencing a similar warming climate, a quantitative relation of their shrinkage to the changing climate will need a good model of the dynamics of avalanche-fed, debris-covered glaciers.

ACKNOWLEDGEMENTS

We acknowledge help from Sri V.K. Raina who kindly provided us with sketch maps of Satopanth and Bhagirath Kharak glaciers. We thank G.S. Badwal, S.S. Badwal, K. S. Sajwan, Praveen Kumar, K. Siddharth and people of Mana village for help during the fieldwork. We also thank the reviewers and editors whose comments helped us to substantially improve the paper.

REFERENCES

- Adhikari S and Huybrechts P (2009) Numerical modelling of historical front variations and the 21st-century evolution of glacier AX010, Nepal Himalaya. *Ann. Glaciol.*, **50**(52), 27–34 (doi: 10.3189/172756409789624346)
- Banerjee A and Azam MF (2016) Temperature reconstruction from glacier length fluctuations in the Himalaya. *Ann. Glaciol.*, **57**(71) (see paper in this issue) (doi: 10.3189/2016AoG71A047)
- Banerjee A and Shankar R (2013) On the response of Himalayan glaciers to climate change. *J. Glaciol.*, **59**(215), 480–490 (doi: 10.3189/2013JoG12J130)
- Basnett S, Kulkarni AV and Bolch T (2013) The influence of debris cover and glacial lakes on the recession of glaciers in Sikkim Himalaya, India. *J. Glaciol.*, **59**(218), 1035–1046 (doi: 10.3189/2013JoG12J184)
- Bhambri R and Bolch T (2009) Glacier mapping: a review with special reference to the Indian Himalayas. *Progr. Phys. Geogr.*, **33**(5), 672–704 (doi: 10.1177/0309133309348112)
- Bhambri R, Bolch T, Chaujar RK and Kulshreshtha SC (2011) Glacier changes in the Garhwal Himalaya, India, from 1968 to 2006 based on remote sensing. *J. Glaciol.*, **57**(203), 543–556 (doi: 10.3189/002214311796905604)
- Bolch T and 11 others (2012) The state and fate of Himalayan glaciers. *Science*, **336**, 310–314 (doi: 10.1126/science.1215828)
- Dobhal DP and Mehta M (2010) Surface morphology, elevation changes and terminus retreat of Dokriani Glacier, Garhwal Himalaya: implication for climate change. *Himalayan Geol.*, **31**(1), 71–78
- Dobhal DP, Mehta M and Srivastava D (2013) Influence of debris cover on terminus retreat and mass changes of Chorabari Glacier, Garhwal region, central Himalaya, India. *J. Glaciol.*, **59**(217), 961–971 (doi: 10.3189/2013JoG12J180)
- Dyurgerov MB and Meier MF (2005) *Glaciers and the changing Earth system: a 2004 snapshot*. (INSTAAR Occasional Paper 58) Institute of Arctic and Alpine Research, University of Colorado, Boulder, CO
- Fujita K and Nuimura T (2011) Spatially heterogeneous wastage of Himalayan glaciers. *Proc. Natl Acad. Sci. USA (PNAS)*, **108**(34), 14 011–14 014 (doi: 10.1073/pnas.1106242108)
- Ghosh J K and Dubey A (2008) India's new map policy: utility of civil users. *Curr. Sci.*, **94**(3), 332–337
- Heim A and Gansser A (1939) Central Himalaya: geological observations of the Swiss Expedition, 1936. *Mem. Soc. Helv. Sci. Natur.*, **73**(1), 76–78

- Immerzeel WW, Van Beek LP and Bierkens MF (2010) Climate change will affect the Asian Water Towers. *Science*, **328**, 1382–1385 (doi: 10.1126/science.1183188)
- Jangpangi BS (1956) Sketch of the snouts of Bhagirath Kharak Glaciers. *Geol. Surv. India*, Sept., 10–14
- Kargel JS, Cogley JG, Leonard GJ, Haritashya U and Byers A (2011) Himalayan glaciers: the big picture is a montage. *Proc. Natl Acad. Sci. USA (PNAS)*, **108**(36), 14 709–14 710 (doi: 10.1073/pnas.1111663108)
- Leclercq PW and Oerlemans J (2012) Global and hemispheric temperature reconstruction from glacier length fluctuations. *Climate Dyn.*, **38**(5–6), 1065–1079 (doi: 10.1007/s00382-011-1145-7)
- Moon T and Joughin I (2008), Changes in the ice front position in Greenland tidewater glaciers from 1992 to 2007. *J. Geophys. Res.*, **113**(F2), F02022 (doi: 10.1029/2007JF000927)
- Mumm AL (1909) *Five months in the Himalaya: a record of mountain travel in Garhwal and Kashmir*. Longmans Green, London
- Nainwal HC and 6 others (2007). Chronology of the Late Quaternary glaciation around Badrinath (Upper Alaknanda basin): preliminary observations. *Curr. Sci.*, **93**(1), 90–96
- Nainwal HC, Negi BDS, Chaudhary M, Sajwan KS and Gaurav A (2008) Temporal changes in rate of recession: evidences from Satopanth and Bhagirath Kharak glaciers, Uttarakhand, using Total Station Survey. *Curr. Sci.*, **94**(5), 653–660
- Oerlemans J (2001) *Glaciers and climate change*. AA Balkema Publishers, Rotterdam
- Oerlemans J (2005) Extracting a climate signal from 169 glacier records. *Science*, **308**(5722), 675–677 (doi: 10.1126/science.1107046)
- Raina VK (2009) Himalayan glaciers: a state-of-art review of glacial studies, glacial retreat and climate change. (MoEF Discussion Paper, Ministry of Environment and Forests, Government of India) G.B. Pant Institute of Himalayan Environment and Development, Kosi Katarmal, Almora
- Raina VK and Srivastava D (2008) *Glacier atlas of India*. Geological Society of India, Bangalore
- Raina VK, Snehamani and Sangewar CV (2015) *Glacier snout monitoring in the Himalayas*. Geological Society of India, Bengaluru
- Sangewar CV (2000) Bhagirath Kharak glacier, Alaknanda basin. *Geol. Surv. India, Rec.*, **135**, 8
- Scherler D, Bookhagen B and Strecker MR (2011) Spatially variable response of Himalayan glaciers to climate change affected by debris cover. *Nature Geosci.*, **4**, 156–159 (doi: 10.1038/ngeo1068)
- Shipton E (1935) Nanda Devi and the Ganges Watershed. *Geogr. J.*, **85**, 305–319
- Smythe FS (1932a) *Kamet conquered*. V. Gollancz, London
- Smythe FS (1932b) Explorations in Garhwal around Kamet. *Geogr. J.*, **79**, 1–11
- Srivastava D (2004) Recession of Gangotri glacier. *Geol. Surv. India Spec. Publ.*, **80**, 21–32
- Survey of India (SOI) (1962) *Topographic map 53/N*. Survey of India, Dehra Dun
- US Army (1954) Topographic map, NH 44-5 (1:250000), Series U502, based on medium scale ground controlled survey during 1924–1943. US Army Corps of Engineers, Washington, DC
- Valdiya KS (1973) Lithological sub-divisions and tectonics of the Central Crystalline Zone of Kumaon Himalaya. In *Proceedings of the Symposium on Geodynamics of the Himalayan region*. National Geophysical Research Institute, Hyderabad, 204–205
- Valdiya KS, Paul SK, Chandra T, Bhakuni SS and Upadhyay RC (1999) Tectonic and lithological characterization of Himadri (Great Himalaya) between Kali and Yamuna rivers, Central Himalaya. *Himalayan Geol.*, **20**(2), 1–17
- Vohra CP (1980), Some problems of glacier inventory in the Himalayas. *IAHS Publ.* 126 (Riederalp Workshop 1978 – *World Glacier Inventory*), 67–74